Marcano, D.; Mauer, G.; Sohn, YJ.; Vaßen, R.; García-Fayos, J.; Serra Alfaro, JM. (2016). Controlling the stress state of La1−xSrxCoyFe1−yO3−δ oxygen transport membranes on porous metallic supports deposited by plasma spray¿physical vapor process. Journal of Membrane Science. 503:1-7. doi:10.1016/j.memsci.2015.12.029.

Controlling the Stress State of $La_{1-x}Sr_xCo_yFe_{1-y}O_{3-\delta}$ Oxygen Transport Membranes Deposited on Porous Metallic Supports by Means of Plasma Spray-Physical Vapor Deposition.

D. Marcano[a], G. Mauer[a], Y. J. Sohn[a], R. Vaßen[a], J. Garcia-Fayos[b], J.M. Serra[b]

[a]Forschungszentrum Jülich GmbH, Institute of Energy and Climate Research-IEK-1, Jülich – Germany
[b]Instituto de Tecnología Química (Universitat Politècnica de València - *Consejo Superior de Investigaciones Científicas*) Valencia - Spain

Abstract

$La_{0.58}Sr_{0.4}Co_{0.2}Fe_{0.8}O_{3-\delta}$ (LSCF), deposited on a metallic porous support by plasma spray-physical vapor deposition (PS-PVD) is a promising candidate for oxygen-permeation membranes. However, after O_2 permeation tests, membranes show vertical cracks leading to leakage during the tests. In the present work, one important feature leading to crack formation was identified. More specifically; Membrane residual stress changes during thermal loading were found to be related to a phase transformation in the support. In order to improve the performance of the membranes, the metallic support was optimized by applying an appropriate heat treatment. The observed oxygen fluxes during permeation tests had infinite selectivity and were amongst the highest fluxes ever measured for LSCF membranes in the thickness range of 30 μm, supported by LSCF porous substrates.

Keywords: Residual Stress, Oxygen transport membrane, Perovskite, Plasma Spray-Physical Vapor Deposition, O_2 permeation test.

1. Introduction

Perovskite structure materials used in membrane systems with applications in oxygen separation modules are the most promising layer materials. They are mixed electronic ionic conductors which allow oxygen diffusion via oxygen vacancies in the crystal lattice. The driving force for the transport is the oxygen partial pressure $p(O_2)$ gradient across the membrane [1, 2]. The oxygen permeation flux across the membrane increases by decreasing the membrane thickness. Therefore, producing a thin perovskite membrane on a porous substrate would improve the permeation flux.

Membranes can be manufactured by different processing routes such as tape casting or screen printing [3, 4]. Plasma spray – physical vapor deposition (PS-PVD) is performed at very low pressures (1 mbar). The low pressure allows the plasma plume to achieve a length of more than 1.5 m and a diameter of 200-400 mm. For the present application, with an electric input power of approximately 90 kW, the vaporization degree of the feedstock can be limited and a splat-like instead of a vapor deposition is obtained. In this way, very thin and dense coatings can be produced [5, 6] . In the PS-PVD process, powder particles are injected into the plasma. Heat transfer from the plasma to the particles is optimized to achieve the maximum degree of melting. Molten particles encounter the substrate with very high kinetic energy; they solidify producing a lamellar microstructure. The splats show a high flowability and are spread widely to form a dense coating closing the gaps of porous materials. Metallic porous supports are suitable for PS-PVD applications because of their stiffness and mechanical strength under depositing conditions. Additionally, they show suitable mechanical properties and can be welded to provide easy module assembly [7].

NiCoCrAlY alloys are usually employed as corrosion resistant coatings or as bond coatings

in gas turbine applications [8]. They show good chemical compatibility with perovskites in the operating temperature range. Also, their coefficient of thermal expansion is similar which should lead to low thermal mismatch stresses. However, coatings can be subjected to residual stresses due to the deposition process, sintering or crystallization or mechanical loading [9].

In the present work, the stress states in an LSCF membrane deposited by PS-PVD on a porous NiCoCrAlY support are analysed in order to explain the appearance of segmentation cracks occurring during O_2 permeation tests. Phase transformation in the support during annealing tests is studied in connection with residual stress changes of the membrane.

2. Experimental

2.1. Metallic porous substrates

Substrates were provided by GKN sinter metals (Radevormwald Filters, Germany). They were fabricated using Amdry 386 NiCoCrAlY powders (Oerlikon Metco, Westbury, NY) with spherical morphology and nominal mean particle diameter of 90 μm. The desired porosity of approximately 35% was achieved via gravity sintering in an argon atmosphere at 400 Torr. The sintering temperature was 1180°C for 150 minutes. The samples obtained were disks 105 mm in diameter and 2 mm thick. The roughness of the samples on the die side was R_a= 7 μm. The PS-PVD coating was deposited on this side. A waterjet cutting device was used to obtain samples with a diameter of 15mm.

2.2. Deposition of the LSCF coating by PS-PVD

The coating was deposited by a Sulzer Metco - Multicoat system (Oerlikon Metco, Wohlen, Switzerland) with an O3CP torch. The feedstock material was the perovskite

$La_{0.58}Sr_{0.4}Co_{0.2}Fe_{0.8}O_{3-\delta}$ (LSCF) provided by Oerlikon Metco. The powder was 93% rhombohedral and 7% orthorhombic as determined by a Rietveld refinement of X-ray diffraction (XRD) patterns. The particles showed a spherical morphology and their sizes were measured by laser diffraction as d_{10} = 6 μm, d_{50} = 10 μm, and d_{90} = 16 μm. The plasma spray parameters used to obtain samples with dense membranes are shown in Table 1. In addition, during spraying, various extra amounts of oxygen gas were supplied to the chamber in order to account for LSCF stoichiometry under reducing conditions.

Table 1: LSCF Coating Parameters.

Parameter	**Dense Membrane**
Plasma gas composition	110 slpm Ar / 20 slpm He
Current	2100 A
Input power	90 kW
Chamber pressure	250 Pa
Powder feed rate	20 g/min
Spray distance	1000 mm
Coating time	3-5 min

slpm: standard liters per minute

2.3. Phase determination in the metallic porous support and in the LSCF coating

X-ray diffraction (XRD, D4 Endeavor - Bruker AXS) and scanning electron microscopy (Ultra 55, Zeiss - Germany) with energy-dispersive microanalysis (EDS) (INCA, Oxford instruments – Germany) were performed to determine the phases present in the metallic porous support and the LSCF coating. XRD measurements were carried out using CuKα radiation (λ=1.5418 Å). The diffraction data were collected between 10° and 140° in 2θ (Δ=0.02°, 2 s/step) with a tube voltage and current of 40kV and 40mA, respectively. The TOPAS V 4.2 software [10] was used on the measured data for the Rietveld analysis.

Also, phase transformation in the metallic porous support during heating was determined in a dilatometry experiment (DIL 402C, Netzsch) and a differential scanning calorimetry (DSC) test.

2.4. O_2 permeation tests

Gas tightness of the tested LSCF samples was checked prior to assembly in the reactor. Permeation tests were performed in a lab-scale quartz reactor. Dilutions of O_2 in N_2 were fed in on the porous support side while Ar as sweep gas contacted the opposite membrane side. Gas leak-free conditions were ensured by monitoring the nitrogen concentration in the permeate gas stream. Similar procedure was already used and it is described in [11]. The data reported here were obtained at steady state after 1 hour in operation. In order to improve oxygen permeation, a 15 μm porous catalytic layer consisting of $Ba_{0.5}Sr_{0.5}Co_{0.8}Fe_{0.2}O_{3-\delta}$ + 5% wt. Pd was deposited on top of the LSCF membrane. This layer was applied by the screen-printing technique including a pore-former in the ink. After layer deposition, it was dried at 80 ºC for 1 hour and then sintered in situ in the experimental set-up.

3. Results and Discussion

3.1. Phases present in the NiCoCrAlY porous support

During O_2 permeation tests, the sample underwent heat treatment that consisted of isothermal steps lasting 3 hours or more. The heat treatment caused segmentation cracks in the membrane (Figure 1). The heat treatment caused a phase transformation in the support, inducing a volume expansion, which changed the residual stress state in the membrane. XRD analyses (Figure 2a), carried out on the porous NiCoCrAlY support showed that the

main phases present were the γ and β phase. In addition, the porous support showed a tetragonal sigma (σ) phase. SEM-EDS analysis (Figures 2b and 2c) confirmed that this was a Co-Y rich σ–phase. During spraying, the heating rate as well as the high temperature experienced by the support did not affect the phase composition of the support. Changes in time due to temperature exposure were negligible when compared to prolonged heat treatments during a permeation test. That is to say, after spraying, the σ phase was still present. In Figure 2a, the XRD pattern of the porous NiCoCrAlY sample after a prolonged heat treatment in air is also shown. The main difference between the 'as-sintered' and 'as-annealed' sample was the σ phase.

3.2. Dilatometry measurements of porous NiCoCrAlY supports

DSC measurements confirmed a phase transformation of the porous metallic support during heating. As can be observed in Figure 3a, the NiCoCrAlY porous support showed a phase transformation at 592 and 709°C. These peaks could correspond to the dissolution of the σ phase into the γ and/or β phase, depending on the Co concentration, in agreement with thermodynamic calculations carried out with Thermocalc [12]. The dilatometry measurement shown in Figure 3b shows the one-dimensional percentile expansion as a function of temperature for the porous NiCoCrAlY sample. It indicates that the sample experienced different thermal expansion behavior when annealing a first ('as-sintered' support) and a second successive time ('as-annealed' support).

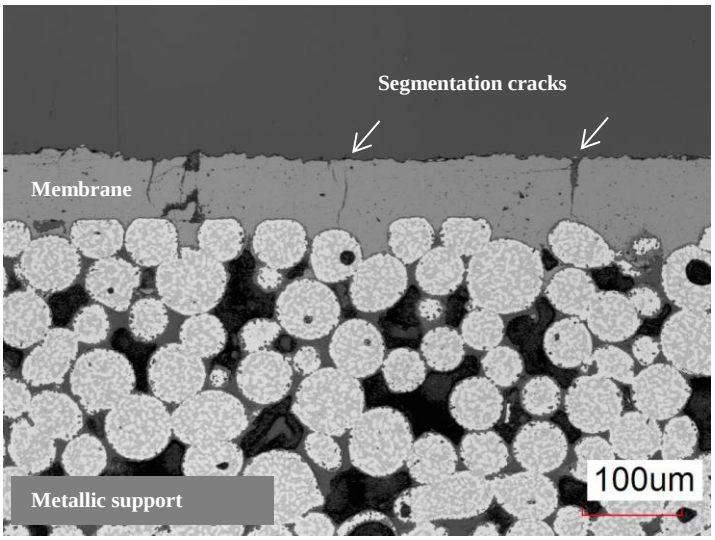

Figure 1: Laser confocal microscope image of LSCF dense membrane on a NiCoCrAlY porous support after annealing of the 'as-sprayed' state. Segmentation cracks were formed in the membrane.

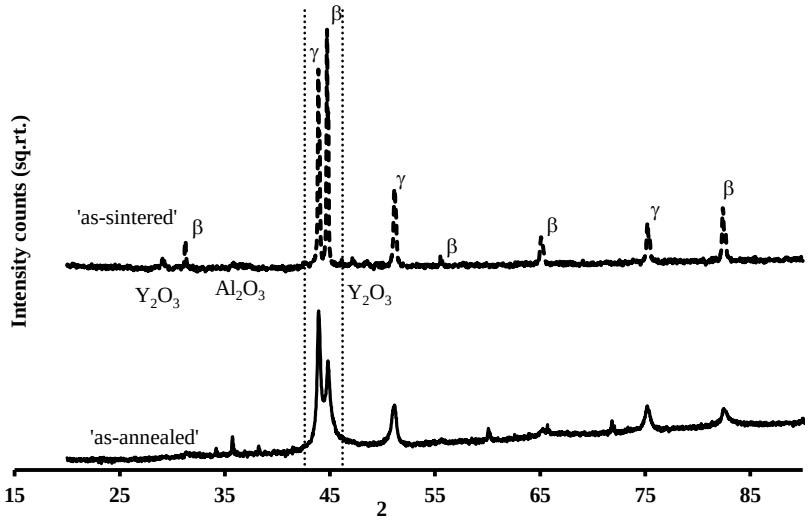

a) XRD pattern of the NiCoCrAlY porous support: 'as-sintered': Identified phases were the γ, β and also a tetragonal σ phase. 'as-annealed': had only the γ and β phases.

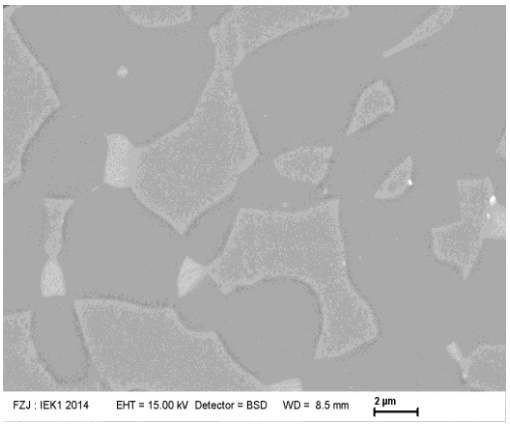

b) SEM (BSE) image of a NiCoCrAlY particle: Dark and light grey regions corresponded to the β and γ phase, respectively. White areas corresponded to the σ phase regions. Small white points at grain boundaries corresponded to Y-Hf-Si

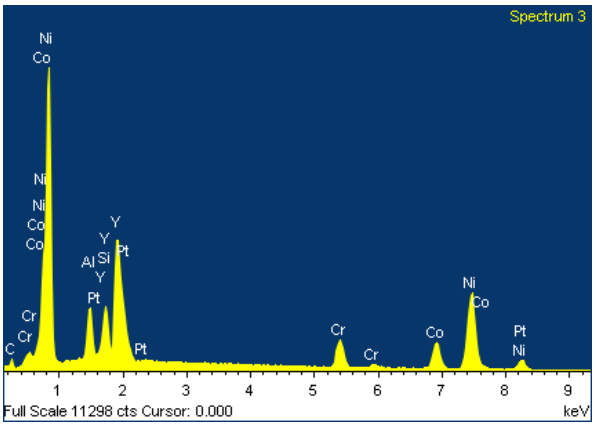

c) The EDS pattern of white regions in showed a Co-Y rich σ phase.

Figure 2: Phases present in the NiCoCrAlY porous support.

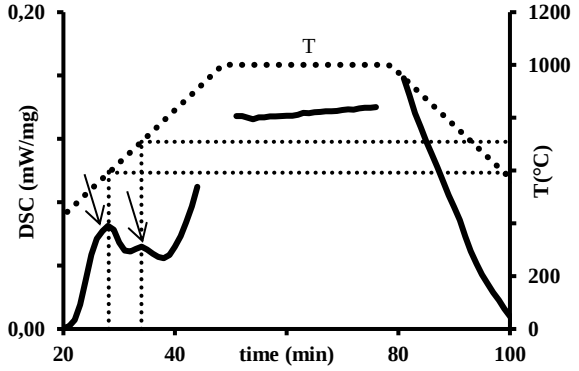

a) DSC results of a porous NiCoCrAlY support. During heating there was a phase transformation at 592.2 and 708.7°C.

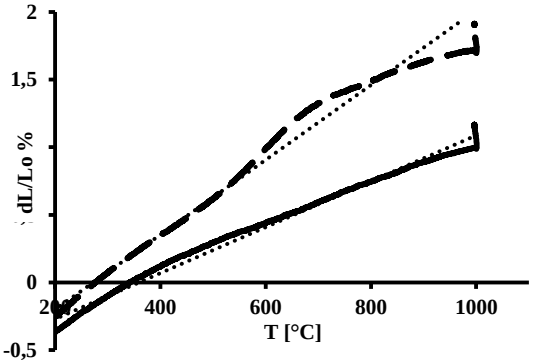

b) Percentile expansion of porous NiCoCrAlY samples as function of temperature. First measurement (- -) (as-sintered) sample. Second successive measurement (-) (as-annealed) sample. The dotted lines are a guide for the eyes.

Figure 3: Measurements indicating a phase transformation in the NiCoCrAlY porous support during heating.

During the first heat treatment, the thermal expansion reached up to 2% at 1000°C. It is to be noticed that the thermal expansion was not linear between 600 and 1000°C with a 'peak'

between 600-800°C. During the second heat treatment, the thermal expansion reached up to 1% at 1000°C and it was linear during the whole temperature range. A similar effect was observed in the coefficient of thermal expansion of a NiCoCrAlY alloy [13]. It was attributed to the dissolution of a γ' into a γ phase. Additionally, in this previous work, the 'peak' was found around 1000°C for a Co-free alloy. The effect of Co was to suppress the formation of the γ' phase and with increasing Co amount the 'peak' was shifted to lower temperatures. Also with increasing Co content, the 'peak' decreased in size. The results were in agreement with this observation. Due to the amount of Co in this alloy, no γ' phase was formed. Instead, a σ-phase was formed with a lower transformation temperature and its 'peak' was shallower than for a Co-free alloy. This led to conclude that dissolution of the σ phase during heat treatment was accompanied with a volume change. At 700°C the volume change ΔV was approximately 5%.

A Rietveld refinement of the XRD pattern in Figure 2a determined the volume of both phases γ and β (Table 2). These indicated that the σ phase dissolved into the γ phase. The volume of the γ phase increased while the volume of the β phase remained unchanged. The volume change in the γ phase accounted for 0.34% at room temperature. Also, the fraction amount of β phase decreased. The density in the γ phase remained unchanged in contrast to the density in the β phase, which changed due to the difference in the site occupancy factors. Therefore, upon annealing, no densification leading to sintering of the porous support took place [14].

Table 2: Density and phase fractions of main and oxide phases in the NiCoCrAlY porous support.

	Phase fraction (%)	Density [gr/cm^3]	V [Å^3]	Site occupancy Factor (Ni)
γ_s	37	8.55(1)	45.58(1)	1
γ_a	59	8.52(1)	45.73(1)	1
β_s	56	5.01(2)	23.53(1)	0.76(1)
β_a	39	4.79(5)	23.50(1)	0.69(1)
σ_s + oxide	7			
σ_a + oxide	2			

'As-sintered' (s) and 'as-annealed' (a). Oxide phases: $Y_2O_3/Cr_2O_3/Al_2O_3$.

3.3. Microstructural changes of porous NiCoCrAlY supports

The σ phase appeared due to the fact that the solubility of Co had reached its limit in the matrix. Image analysis carried out on SEM pictures showed that the amount of sigma phase depended on the particle size. Figure 4a shows this dependency. In the 'as-sintered' support, it is observed that smaller particles have more σ phase per unit area than bigger particles. With increasing temperature, the solubility of Co increased in the γ phase. Therefore, after annealing, the σ phase was diminished for all particle sizes. This was especially the case for the smallest particles with sizes less than 500 μm^2 due to the fact that in smaller grains, the solubility of Co was shifted to a higher limit [15]. As mentioned before, the two peaks observed in the DSC measurement (Figure 3a) corresponded to a phase transformation at 592.2 and 708.7 °C. It has been established that these peaks arose due to the transformation of the σ phase into the γ phase. The two different transformation temperatures were in agreement with the σ amount dependency on particle size.

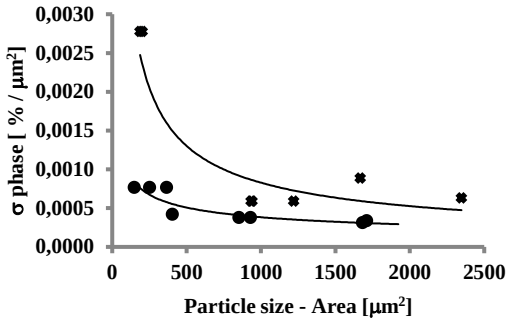

a) σ phase dependency on particle size. Smaller particles had less amount of σ phase in comparison with bigger particles. 'as-sintered' support (x). 'as-annealed' support (●).The lines are a guide for the eyes.

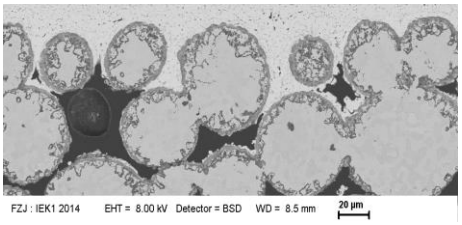

b) SEM image of the NiCoCrAlY porous support after a prolonged permeation test (300 h). No σ phase was present. The β phase was partially transformed into the γ phase. Particles are surrounded by an Al_2O_3 layer

Figure 4: Microstructural changes after annealing in air.

That is to say, particles with sizes less than 500 μm^2 experienced the transformation at lowered temperature than particles with sizes more than 500 μm^2, as the tendency in Figure 4a suggests. This is due to a dependency of transformation enthalpies on surface areas of particles [16].

During annealing, the particles in the porous support underwent microstructural changes not only due to dissolution of the σ phase but also related to changes occurring in the main phases γ and β (Figure 4b). After a prolonged permeation test (approximately 300 h), the σ phase dissolved completely into the γ phase. Some of the Al in the β phase diffused to the particle surface forming an oxide and also a fraction of the β phase transformed into the γ phase. Due to the formation of an oxide layer surrounding the NiCoCrAlY particles, neither lattice diffusion between isolated particles nor surface diffusion towards the necks of the particles occurred. That is to say, the porous support was suitable for prolonged term

operation without sintering, further phase transformations or interdiffusion between the ceramic coating and the metallic support. However, stresses in the membrane arising from the oxide at longer operation terms need to be studied.

3.4. Ceramic coatings deposited on porous NiCoCrAlY supports

As mentioned earlier, when annealing of an 'as-sintered' support, ΔV was approximately 5% at 700°C. Even though ΔV was relatively small, it was enough to generate cracks in the membrane. During heating, the volume expansion experienced by the support led to a change in the residual stress of the membrane into a tensile regime. In order to account for the volume expansion, prior to coating, supports were annealed for 2 hours at 720°C under an argon atmosphere using a Ti getter. After coating, further annealing in air was carried out. Surfaces of coated samples are shown in Figure 5. When the coating is applied to an 'as-sintered' support, annealing in air led to a crack network on the surface and membranes were not gastight. However, if the substrate was annealed prior to coating, there was no longer the appearance of a crack network on the surface when annealing a second time. Even if sequential annealing steps in argon or in air were carried out to coatings deposited on previously annealed supports, the resulting membranes still had a surface without a crack network. This was an indication that the dissolution of the σ phase present in the metallic support played the main role in the cracking phenomena of the membranes. Annealing in Ar would account for phase transformations effects of the support whereas annealing in air would account for oxidation effects of the support. Both effects would generate stresses in the membrane.

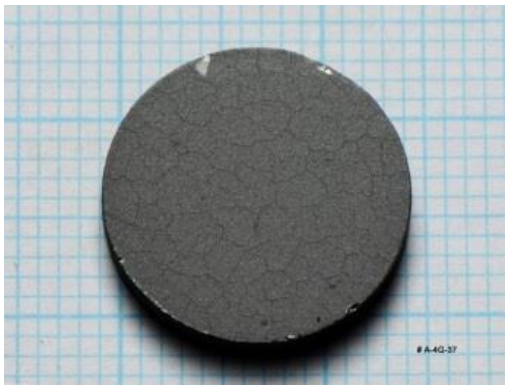

a) Coating on 'as-sintered'

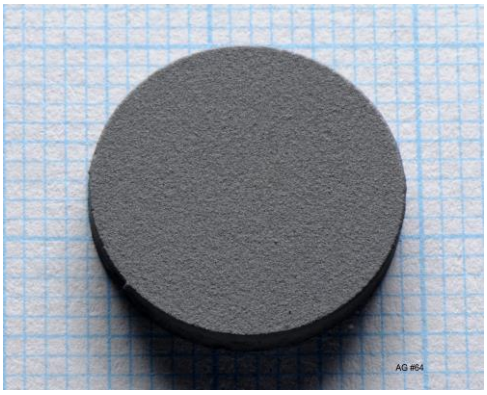

b) Coating on 'as-annealed' support. After annealing in Ar at 900°C .

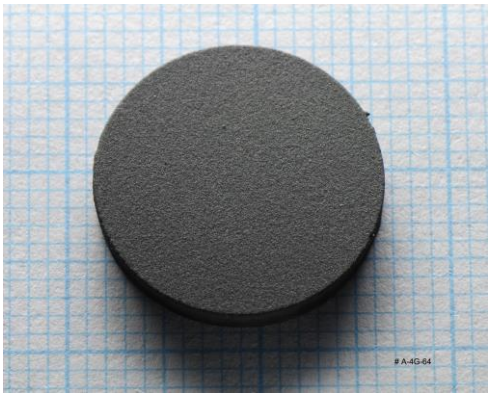

c) Coating on 'as-annealed' support. After annealing in Air at 900°C .

Figure 5: Membrane surfaces after annealing in air.

3.5. O_2 permeation tests

Oxygen permeation tests were performed as a function of temperature (1000-700 ºC), p_{O_2} in feed stream and Ar in the sweep stream. The thermal evolution of oxygen permeation is depicted in Figure 6 and corresponds to samples sprayed with an additional 12 slpm and 16 slpm O_2 flux (samples A and B respectively). The obtained results fit a two-fold Arrhenius behavior. For example, sample A had apparent activation energies (E_a) of 114±4 kJ·mol^{-1} in the range 1000-800 ºC and 160±10 kJ·mol^{-1} in the range 800-700 ºC. This value was ca.

30 kJ·mol^{-1} higher than that previously observed in other all-LSCF asymmetric membranes [17]. This difference could be ascribed to the use of a metallic substrate, and the presence of Al_2O_3 at the support surface of the membrane. The highest oxygen flux J(O_2) was obtained for sample B, at 1000 ºC with a value of 5.3 ml·min^{-1}·cm^{-2}. The observed J(O_2) in the present work was amongst the highest fluxes ever measured for LSCF membranes in the thickness range of 30 μm, which were supported over LSCF porous substrates [17].

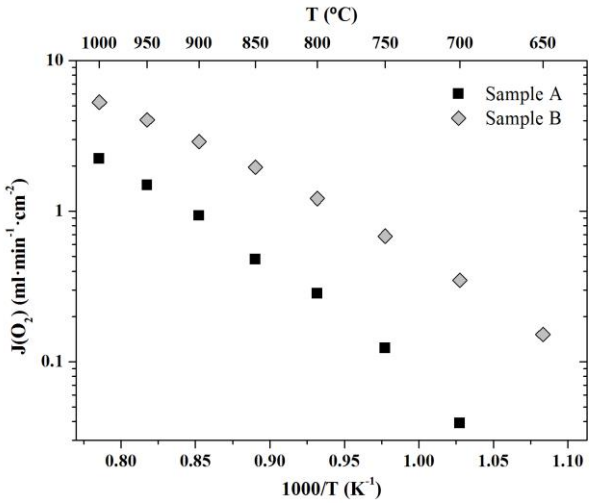

Fig. 6. Oxygen permeation as a function of the temperature under Air/Argon gradient. Synthetic air as feed gas (300 ml·min^{-1}) and Argon as sweep gas (300 ml·min^{-1}).

The reported permeation rates had infinite selectivity. This means that no leakages were registered while the experiments were running. Therefore, no segmentation cracks were formed during experiments with O_2 permeation tests carried out on these structures. Sample B showed a higher permeation rate than sample A. It was assumed that sample B had a higher fraction of perovskite phase than sample A [18] .

The advantage of the PS-PVD method compared to wet chemical methods was that no subsequent sintering procedure is needed to remove organic solvents incorporated in

the coating precursors and to provide cohesion of the membrane layer. In addition, used atmospheres are restricted for metallic supports and their volume changes during heating leads to stresses in the membrane.

4. Conclusions

In this work, the source of stress buildup in metal supported membranes has been identified. During an O_2 permeation test, the heat treatment experienced by the NiCoCrAlY metallic porous support drives a phase transformation with an accompanying volume change. The volume change causes tensile residual stress in the membrane. This is the cause of segmentation cracks during permeation tests. Applying a suitable heat treatment to the supports, prior to coating, controls the stress state in the membrane, during heat treatments.

O_2 permeation fluxes are optimized by obtaining more perovskite and less non-perovskite phases developing during O_2 permeation tests. This feature has been extensively investigated and results are to be published soon.

Dense coatings fabricated by means of PS-PVD are unique and represents a big advantage over other ceramic processing methods.

Acknowledgments

The authors gratefully acknowledge Mr. Ralf Laufs for his help with the use of the PS-PVD facility, the preparation of the SEM and EDS investigations by Dr. Doris Sebold and Mr. P. Terberger for calculations and discussion of Thermocalc phase diagrams (Forschungszentrum Jülich, IEK-1). The work on membranes by PS-PVD was part of the DEMOYS Project funded from the European Community's Seventh Framework Programme, FP7/2007-2013, under grant agreement no. 241309.

References

[1] J. Hong, P. Kirchen, A.F. Ghoniem, Numerical simulation of ion transport membrane reactors: Oxygen permeation and transport and fuel conversion, J. Membr. Sci., 407 (2012) 71-85.

[2] C. Wagner, Equations for transport in solid oxides and sulfides of transition metals, Prog. Solid State Chem., 10 (1975) 3-16.

[3] F. Schulze-Kuppers, S. Baumann, W. Meulenberg, H. Buchkremer, New generation of LSCF oxygen transport membranes, Procedia Eng., 44 (2012).

[4] F. Schulze-Kuppers, S. Baumann, F. Tietz, H.J.M. Bouwmeester, W.A. Meulenberg, Towards the fabrication of $La_{0.98-x}Sr_xCo_{0.2}Fe_{0.8}O_{3-\delta}$ perovskite-type oxygen transport membranes, J. Eur. Ceram. Soc., 34 (2014) 3741-3748.

[5] M.O. Jarligo, G. Mauer, M. Bram, S. Baumann, R. Vaßen, Plasma spray physical vapor deposition of $La_{1-x}Sr_xCo_yFe_{1-y}O_{3-\delta}$ thin-film oxygen transport membrane on porous metallic supports, J. Therm. Spray Technol., 23 (2013) 213-219.

[6] N. Zotov, S. Baumann, W.A. Meulenberg, R. Vaßen, La–Sr–Fe–Co oxygen transport membranes on metal supports deposited by low pressure plasma spraying-physical vapour deposition, J. Membr. Sci., 442 (2013) 119-123.

[7] Y. Xing, S. Baumann, S. Uhlenbruck, M. Ruttinger, A. Venskutonis, W.A. Meulenberg, D. Stover, Development of a metallic/ceramic composite for the deposition of thin-film oxygen transport membrane, J. Eur. Ceram. Soc., 33 (2013) 287-296.

[8] R. Vaßen, M.O. Jarligo, T. Steinke, D.E. Mack, D. Stöver, Overview on advanced thermal barrier coatings, Surf. Coat. Technol., 205 (2010) 938-942.

[9] P.J. Withers, H.K.D.H. Bhadeshia, Overview - Residual stress part 2 - Nature and origins, Mater. Sci. Technol., 17 (2001) 366-375.

[10] Bruker AXS, TOPAS V4, General profile and structure analysis software for powder diffraction data, in, Karlsruhe, Germany, 2008.

[11] C. Gaudillere, J. Garcia-Fayos, J.M. Serra, Enhancing oxygen permeation through hierarchically-structured perovskite membranes elaborated by freeze-casting, J. Mater. Chem. A, 2 (2014) 3828.

[12] J.O. Andersson, T. Helander, L.H. Hoglund, P.F. Shi, B. Sundman, THERMO-CALC & DICTRA, computational tools for materials science, Calphad, 26 (2002) 273-312.

[13] R. Muñoz-Arroyo, D. Clemens, F. Tietz, R. Anton, J. Quadakkers, L. Singheiser, Influence of composition and phase distribution on the oxidation behaviour of NiCoCrAIY alloys, Mater. Sci. Forum, 369-372 (2001) 165-172.

[14] G. Randall, Sintering: from emprirical observations to scientific principles Elsevier, 2014.

[15] B.B. Straumal, A.A. Mazilkin, S.G. Protasova, A.A. Myatiev, P.B. Straumal, B. Baretzky, Increase of Co solubility with decreasing grain size in ZnO, Acta Mater., 56 (2008) 6246.

[16] Nataraja.M, A.R. Das, C.N.R. Rao, Particle Size Effects and Thermal Hysteresis in Crystal Structure Transformations, T Faraday Soc, 65 (1969) 3081.

[17] J.M. Serra, J. Garcia-Fayos, S. Baumann, F. Schulze-Kuppers, W.A. Meulenberg, Oxygen permeation through tape-cast asymmetric all-$La_{0.6}Sr_{0.4}Co_{0.2}Fe_{0.8}O_{3-\delta}$ membranes, J. Membr. Sci., 447 (2013) 297-305.

[18] D. Marcano, G. Mauer, Y.J. Sohn, R. Vaßen, J. Garcia-Fayos, J.M. Serra, The Role of Oxygen Partial Pressure in Controlling the Phase Composition of $La_{1-x}Sr_xCo_yFe_{1-y}O_{3-\delta}$ Oxygen Transport Membranes Manufactured by Means of Plasma Spray - Physical Vapor Deposition, (n.d.).